# Area method compared with Transect method to measure shoreline movement

Sam Khallaghi and Robert Gilmore PontiusJr.

#### **QUERY SHEET**

This page lists questions we have about your paper. The numbers displayed at left are hyperlinked to the location of the query in your paper.

The title and author names are listed on this sheet as they will be published, both on your paper and on the Table of Contents. Please review and ensure the information is correct and advise us if any changes need to be made. In addition, please review your paper as a whole for typographical and essential corrections.

Your PDF proof has been enabled so that you can comment on the proof directly using Adobe Acrobat. For further information on marking corrections using Acrobat, please visit <a href="http://journalauthors.tandf.co.uk/production/acrobat.asp">https://journalauthors.tandf.co.uk/production/acrobat.asp</a>; <a href="https://authorservices.taylorandfrancis.com/how-to-correct-proofs-with-adobe/">https://authorservices.taylorandfrancis.com/how-to-correct-proofs-with-adobe/</a>

The CrossRef database (www.crossref.org/) has been used to validate the references.

#### **AUTHOR QUERIES**

- Q1 Please provide the page range for Addo 2015.
- Q2 Please provide complete details for (Thieler et al. 2009) in the reference list or delete the citation from the text.
- O3 Please provide the publisher location for Burns et al. 2020.
- Q4 Please provide the volume number and page range for Elkafrawy et al. 2020.
- Q5 Please provide the volume number for Jana 2019.
- Q6 Please provide the volume number, page range and journal title for O'Brien et al. 2014; Rooney et al. 2019.
- O7 Please provide publisher name and location for Himmelstoss et al. 2018.
- Please note that the ORCID section has been created from information supplied with your manuscript submission/CATS. Please correct if this is inaccurate.





# Area method compared with Transect method to measure shoreline movement

08 Sam Khallaghi and Robert Gilmore Pontius, Jr. (1)



#### **ABSTRACT**

9

11 12 13

14

15

16

17

18

19

20

21

22

23

24

25

26

31 32

33

34

35

36

37

38

39

40

41

42

43

44

45

46

47

49

Vector GIS represents shorelines as polylines that show the boundaries between land and water. This article compares two methods to measure how boundaries move among time points. The Area method converts the polylines at various time points into polygons of either land or water. The Area method measures temporal change as loss or gain of land areas. The Transect method requires subjective decisions to draw a baseline near the shorelines and then to draw transects that emanate from the baseline to intersect the shorelines. The Transect method measures temporal change as the distance between the intersection points along each transect as in the software packages AMBUR and DSAS. This article compares the conceptual foundations of the two methods. We illustrate how the Area method produces results for cases where the Transect method encounters practical difficulties. We list each method's characteristics, so researchers can align the method with their research question.

#### ARTICLE HISTORY

Received 7 January 2021 Accepted 19 April 2021

#### **KEYWORDS**

AMBUR; boundary movement; coastal studies; DSAS; GIS; shoreline change

#### 1. Introduction

Shorelines are interfaces between the aquatic and terrestrial ecosystems usually distinguished by a topographic gradient along the lateral land-water margin (Dolan et al. 1991; Florsheim et al. 2008). Shorelines can change position through time due to interactions of many physical processes. For instance, sedimentation, erosion, sea-level rise, nearshore currents and human intervention are among the prominent causes of ocean shoreline dynamics (Mukhopadhyay et al. 2012). Similarly, river shoreline dynamics derive from sediment load, biological activity, weather patterns, surface run-off, morphological variability and human intervention (Calow and Petts 1992; Kummu et al. 2008).

Quantifying the rate of movement of shoreline over time and determining its future position can help in coastal engineering by facilitating the modelling of coastal morphodynamics (Boak and Turner 2005; Maiti and Bhattacharya 2009) thus can inform policymaking decisions regarding the management of coastal systems (Pollard et al. 2019). Positional change of river shorelines, also called riverbanks, influences flood-plain habitats and plays an important role in impact assessment models and ecological management (Currin et al. 2015). Therefore, scientists require a method to characterize the amount and rate of temporal change in the positions of boundaries between land and water.

51 52

53 54

55

56

57

58

59

60

61 62

63 64

65

66

67

68

69

70

71

72

73

74

75

76

77

78

79

81

82

83

84

85

86

87

88

89

90

92

93

94

95

96

97

Vector GIS can use polygons to represent areas of land or water, in which case shorelines are the borders between polygons. Alternatively, vector GIS can use polylines to represent shorelines. Each representation requires a distinct method to measure temporal change.

Our article compares approaches to characterize the temporal change of boundaries in a vector GIS based on two representational models: polygons and polylines. The two approaches are the Area method and the Transect method. We articulate the analytic capabilities of each approach in-depth, so that reader can understand how each method addresses its particular goal.

The literature contains two major types of quantitative methods to study shoreline dynamics. Numerical models are usually complex and require a variety of hard-to-collect data to model the shoreline evolution based upon the impact of morph-dynamic processes on the coastal system. Numerical models are often site-specific and their parameters need recalibration before they can be applied to a different geographical setting (Zeinali et al. 2020). Increase in availability of remotely sensed data and maturity of shoreline extraction techniques have led to the increasing popularity of GIS methods in shoreline change analysis. A good example is CoastSat, which automates the extraction of shorelines from the Landsat and Sentinel-2 archive in Earth Engine (Vos et al. 2019). Regardless of whether portraying a shoreline as borders between polygons or as polylines, such models formulate the change as accretion or erosion with the assumption that historical position of the shoreline is a good representative of the aggregation of all the processes that impact the coast through time (Dolan et al. 1991; Currin et al. 2015).

Our literature search found a few articles that used the Area method based on polygons. Fearnley et al. (2009) explored the impact of a tropical cyclone on Chandeleur Islands shorelines in Louisiana. They use both Area and Transect methods to measure changes of shoreline in terms of area and distance, and then related the changes to hurricane frequency and storm intensity. Yao et al. (2011) used pairwise polygon overlay to assess the shape and positional change in China's Yellow River from 1958 to 2008 and report the rate of accretion and erosion for each riverbank. Sarwar and Woodroffe (2013) used the Area and Transect methods to analyse Landsat-derived shorelines at 1989 and 2009 in Bangladesh. Deabes (2017) used the Area and Transect methods to analyse the shoreline change along the Nile delta coast between 1970 and 2010 using twelve time points. Dewan et al. (2017) analysed the evolution of the Ganges and Padma riverbanks within Bangladesh from 1973 to 2011 using both Area and Transect methods. Langat et al. (2019) studied the dynamics of the Tana river in Kenya from 1975 to 2017 using the Area method after extracting the riverbanks from Landsat imagery.

We found more articles that used the Transect method than the Area method. Dolan et al. (1991) used data from a 65 km section of North Carolina to estimate the rate of change and potential sources of error. They reported that various parameterizations of the Transect method caused larger variation in rates where the shoreline curved more. To and Thao (2008) used the Transect method as implemented in the Digital Shoreline Analysis System (DSAS) package to quantify the rate of shoreline change in Nam Dinh, Vietnam. They quantified change using four methods: Endpoint rate (EPR), Average of Rates (AOR), Linear Regression (LRR) and Jack-Knife rate (JKR). The rate of change was similar for EPR & AOR and LRR & JKR, while there was a substantial 10 m/year difference between the two pairs of methods. The authors reported difficulty in drawing nonintersecting transects near the river mouth. Kuleli et al. (2011) introduced an automated methodology using histogram-based segmentation of Landsat imagery to classify land and water in Turkey. They fed polylines into DSAS to compute the rate of change using weighted linear regression and endpoint rate methods. In a similar study, Kankara et al. (2014) used DSAS to capture the rate of change along a part of the Chennai coast in India from 1990 to 2013. Beetham and Kench (2014) examined shoreline dynamics during three weeks in June 2010 at the Vabbinfaru coral reef platform in the Maldives. They defined the shoreline as the toe of the beach, and then mapped the shoreline at three time points. They defined a circular baseline using a buffer around the centroid of a polygon that showed the edge of vegetation. They then extended transects in one-meter intervals from the baseline and used DSAS 4.3 to capture the variations in shoreline position. Roy et al. (2018) used High Water Line (HWL) as shoreline definition and Modified Normalized Difference Water Index (MNDWI) as a means for extracting shorelines of Odisha coast from 1990 to 2015. Extracted shorelines are then processed using DSAS to report long-term rate of change. Jana (2019) used the DSAS package to study the spatio-temporal variability of riverbanks along a 155 km segment of the Subarnarekha River. They reported the rate of change for each bank and reported an overall positional accuracy of around 0.05 m for the evaluation of the short term prediction of riverbank position. Ciritci and Türk (2019) extracted shorelines of Göksu delta from Landsat 5 and analysed the rate of change using DSAS for the period between 1984 and 2011 using six time-points. Elkafrawy et al. (2020) used eight shorelines from 1973 to 2018 and the DSAS package to explore the effectiveness of coastal protective structures in Egypt. Zagórski et al. (2020) used DSAS to study the dynamics of the Calypsostranda shoreline in the period of 2007 to 2017 including both short-term and multidecadal trends to the produce shoreline hazard map of the area.

Jackson et al. (2012) developed an R package called Analyzing Moving Boundaries Using R (AMBUR), which uses an implementation of the Transect method to quantify the rate of change in a time series of shorelines. AMBUR provides some new functions such as near transects that can partially solve the problem of crossing transects in highly curved shorelines. AMBUR also provides some graphical tools that do not exist in DSAS. Addo (2015) used AMBUR to explore the trends of shoreline change among five time points in Ghana. Eulie et al. (2013) used AMBUR to analyse sub-annual shoreline changes in North Carolina. Zhu et al. (2014) adopted the average high-tide line as the definition of shoreline. They used AMBUR to describe the change in terms of distances. They also studied the variations in the coastline length and change in the sea area. Jayson-Quashigah et al. (2019) studied sediment budgets in Ghana. Wiberg et al. (2019) used AMBUR to compare the rate of shoreline change in shallow coastal bays across three time points: 2006, 2009 and 2014. Various non-academic organizations also use the Transect method to describe change in coastal areas (O'Brien et al. 2014; Bracewell 2017). We have not found literature that compares conceptually the Area method to the Transect method. We have not found literature that reports when either method fails to produce interpretable results. Meanwhile, we have encountered cases where the Transect method fails to produce results due to conceptual challenges with the Transect method. This is the motivation for us to write this article. The 'Methods' section describes both methods. The 'Results' section summarizes our findings in a table that compares the methods. The 'Discussion' section elaborates on the findings. The 'Conclusion' section summarizes how each method has a distinct conceptual foundation and goal.

#### 2. Materials and methods

99

100

101

102

103

104

105

106

107

108 109

110

111

112

113

114

115

116

117

118

119

120

121

122

123

124

125

126

127

128

129

130

131

132

133

134

135

136

137

138

139

140 141 142

143

144 145

146

147

## 2.1. Materials for the Plum Island Ecosystems

We illustrate the concepts with an example from the Plum Island Ecosystems (PIE), which is a site of the Long-Term Ecological Research network of the United States National Science Foundation. The PIE site is a marsh-dominated estuary in northeastern

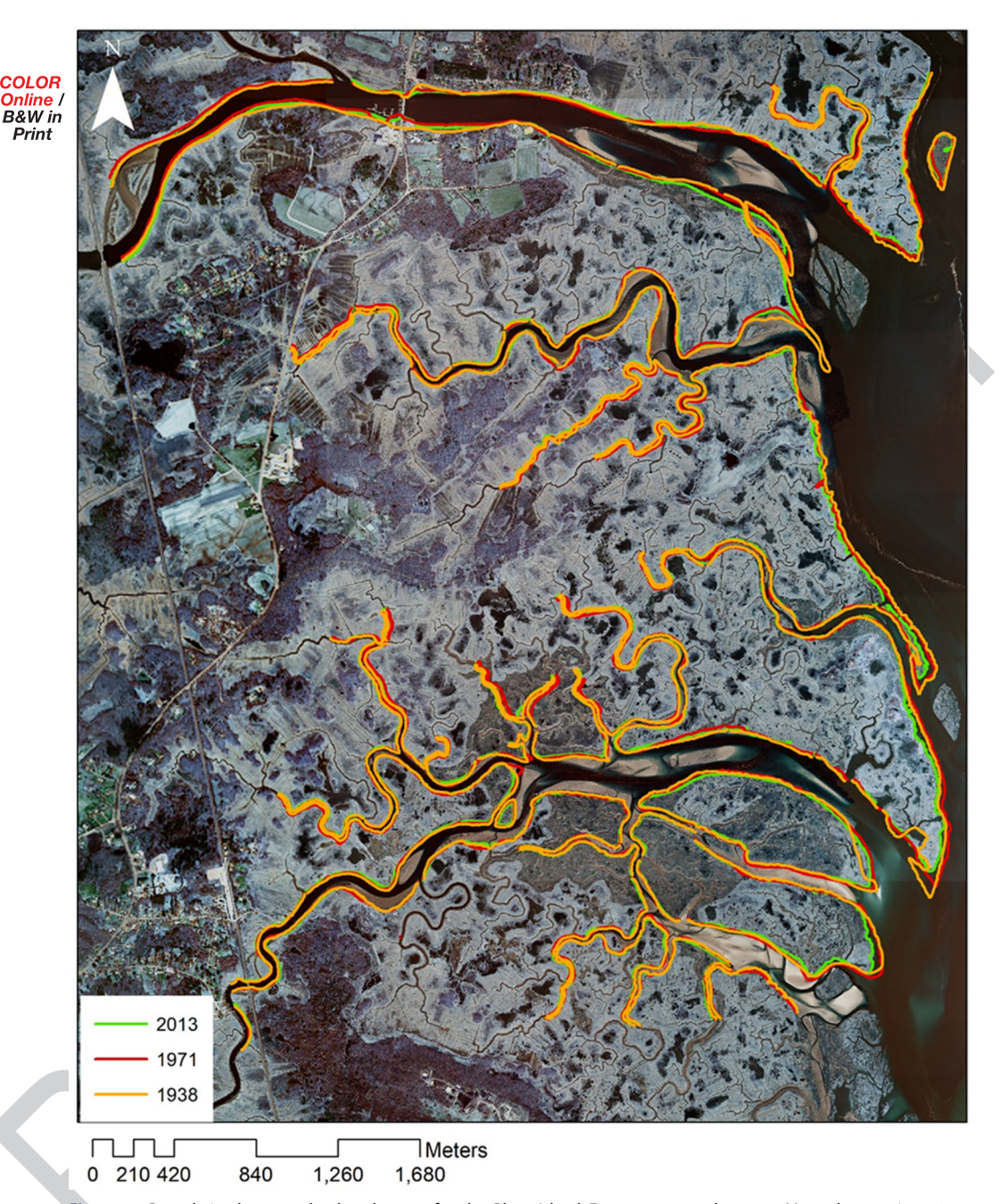
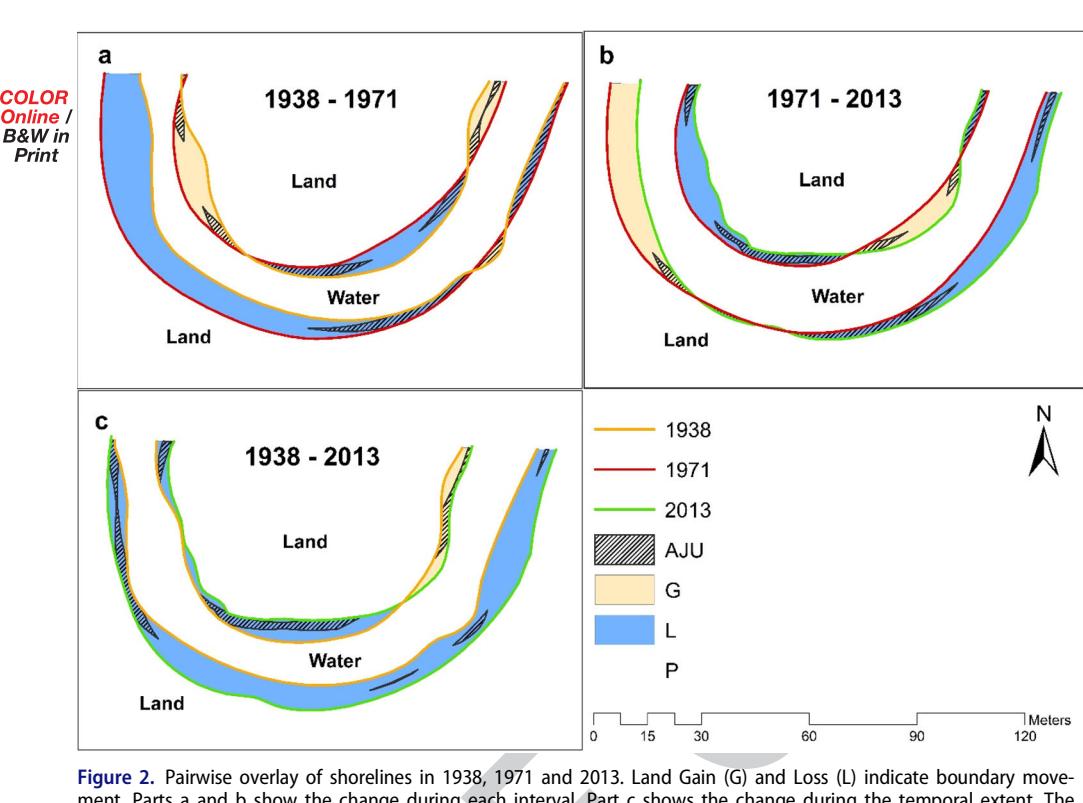


Figure 1. Boundaries between land and water for the Plum Island Ecosystems, northeastern Massachusetts in 1938, 1971 and 2013.

Massachusetts, USA. Figure 1 shows the data, which consist of polylines that separate land from water at three time points: November 1938, July 1971 and April 2013. The spatial extent consists mainly of brackish and saline marshes with elevation ranges between sea level and 2 metres (Hopkinson et al. 2018). The riverbanks were digitized as polylines, using a heads-up method on a Wacom tablet. Information on the PIE dataset is in Burns



ment. Parts a and b show the change during each interval. Part c shows the change during the temporal extent. The shaded part of transition polygons shows the area of joint uncertainty (AJU) based on the reported positional uncertainty of the shoreline polyline.

et al. (2020). The recorded positional accuracy for each time point in chronological order is 3.07, 2.85 and 2.74 metres, which are assumed constant for the entire length of shoreline. According to the dataset metadata, 'The positional accuracy was assessed using the method described in Rooney et al. (2009). Sources of error were identified and summed in quadrature at each year. Digitizer error was assessed by repeatedly digitising the same location five times and taking the standard deviation of the shoreline position'.

We illustrate the two methods using subsets of the shoreline dataset that have continuous shorelines at three time points: 1938, 1971 and 2013. Figure 2 shows an overlay for each of the three time intervals: 1938-1971, 1971-2013 and 1938-2013. Land experiences loss and gain during each of the time intervals. Figure 2(a) shows that the river moves mostly to the west during 1938-1971. Figure 2(b) shows that the river moves mostly to the east during 1971-2013. Figure 2(c) shows that the river widens during 1938-2013.

#### 2.2. Methods

#### 2.2.1. Area method

Figure 3 shows the steps to perform the Area method. We assume the original data are polylines. If discontinuous polylines portray a shoreline, then the first step connects the gaps between the polylines to form a continuous polyline. If the gaps are small, then the gap-filling algorithms in GIS packages such as ArcGIS and QGIS can connect the gaps. Filling large gaps requires a new extraction of shorelines or a different selection of the

247

248

249 250 251

252

253

254

255

256

257 258 259

260

261

266

267

268

269

274

275

276 277

278

279

280

281

282

283 284

285

286

287 288 289

290

291

292 293 294

**Figure 3.** Flow diagram of steps for Area method. Rectangles indicate the required steps. Rectangles with curved sides show outputs.



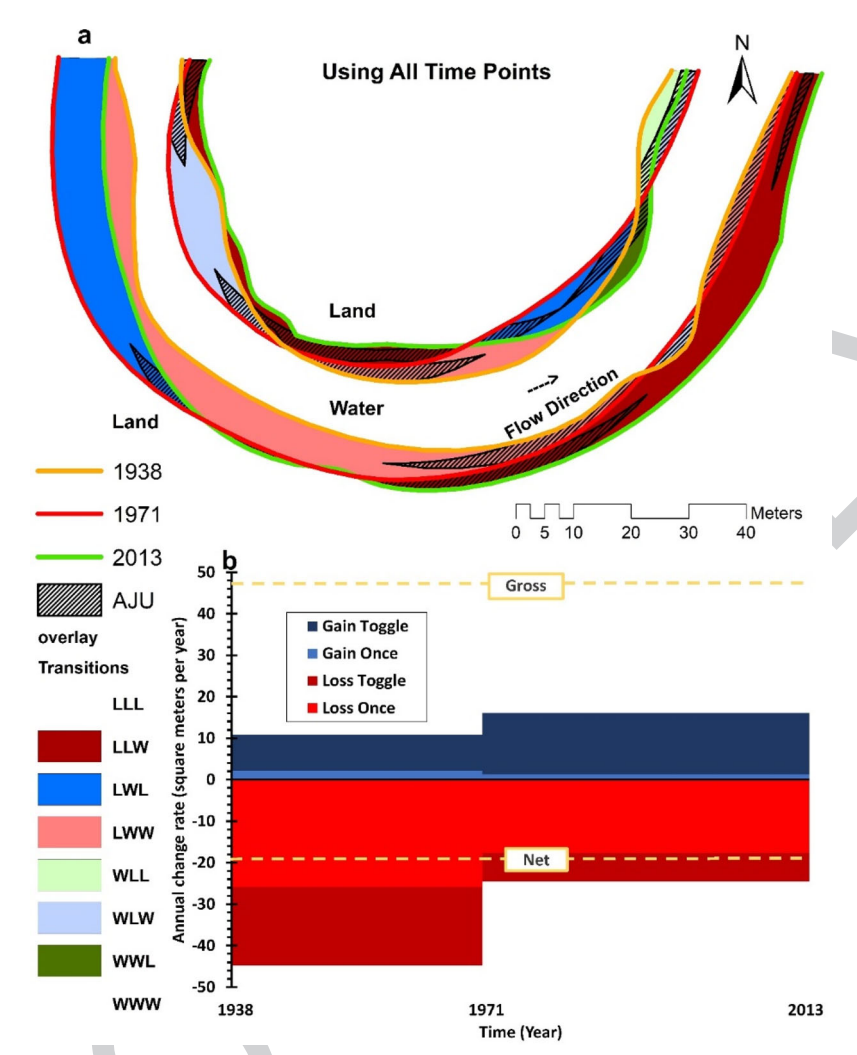


Figure 4. Gains and losses during two time intervals. Part 'a' shows the output of the Area method on a river for three time points. L denotes land, W denotes water, and the three-letter code indicates the sequence of three time points, for example, LWL denotes land in 1938, water in 1971, and land in 2013. The Area of Joint Uncertainty (AJU) is shown with cross-hatched polygons. Part b shows stacked bars that indicate annual change. The width of the bar is the duration of each time interval. The total height of the stacked bars indicates the annual change during each time interval. The bars' segments show specific land transitions. Gain Once segments are WLL for the first time interval and WWL for the second time interval. Gain Toggle segments are WLW during the first time interval and LWL during the second time interval. 'Loss Once' segments are LWW during the first time interval and LLW during the second time interval. The 'Loss Toggle' segments are LWL during the first and WLW during the second time interval. The area of 'Gain Toggle' during 1938-1971 is identical to the area of 'Loss Toggle' during 1971-2013. Area of 'Loss Toggle' during 1938-1971 is identical to the area of 'Gain Toggle' during 1971-2013.

spatial extent. A bounding polygon allows the GIS to use continuous polylines to generate polygons within the bounding polygon. The continuous polylines at each time point stratify the bounding polygon into polygons of either land or water. The maps at the various time points are then overlaid in the GIS system to generate sub-polygons, where each sub-polygon shows a temporal sequence of land or water.

Figure 4 illustrates an application of the Area method. If T denotes the number of time points, then  $2^T$  is the number of possible sequences between land and water during

345

346

347

348

349

350

351

352

353 354

355

356

357 358

359

360

361 362

363

364

365

366

367

368

369

370

371

372

373

374

375

376

377

378

379

380

381

382

383

384

385

386

387

388

389

390

391

392

T-1 time intervals. Figure 4(a) uses the letter L to denote land and the letter W to denote water at each time point. The eight sequences across the three time points are LLL, LLW, LWL, LWW, WLL, WLW, WWL and WWW. LLL and WWW are persistence during both time intervals. LLW is the land's persistence then loss. LWL is land's loss then gain. LWW is land's loss then water's persistence. WLL is land's gain then persistence. WLW is land's gain then loss. WWL is water's persistence then land's gain. LLW and LWW show land loss during the temporal extent. Analogously, WLL and WWL show land gain during the temporal extent.

The segmented bar graph in Figure 4(b) shows four sequences of change. The width of each segment is proportional to the duration of each time interval. The vertical axis is annual change; thus, the area of each bar segment is proportional to the area of change in the polygons of the map in Figure 4(a). The height of the stacked bar is the annual gross change during each time interval. Figure 4(b) shows the first time-interval has a faster annual change compared to the second time interval. The two segments above the horizontal axis show land's gain during each time interval, while the two segments with negative change rates below the horizontal axis show land's loss. The green segments of 'Gain Once' are land's gain then persistence during the first time interval and water's persistence then land's gain during the second time interval. The yellow segments with a densely dotted pattern of 'Gain Toggle' are land's gain then loss during the first time interval and land's loss then gain during the second time interval (Pontius et al. 2017). The red segments of 'Loss Once' are the areas of land loss then water persistence during the first time interval and land's persistence then loss during the second time interval. The yellow segments with sparse dot patterns of 'Loss Toggle' are land's loss then gain during the first time interval and land's gain then loss during the second time interval. The stacked bar shows land's loss is greater than land's gain during both time intervals, as the sum of the sizes of the negative segments is larger than the sum of sizes of the positive segments during each time interval. The Net line is land's annual net change during the temporal extent, which is the Gain segments minus the loss segments scaled by the segments duration divided by the total duration of the temporal extent. The Gross line is land's annual gross change during the temporal extent, which is the Gain segments plus the loss segments divided by the duration of the temporal extent.

The position of the shoreline contains uncertainty due to seasonality, environmental conditions, georeferencing errors and various semantics of shoreline definition (Wernette et al. 2017). The validity of the estimated rate of land change depends upon whether the shoreline movement exceeds the polyline uncertainties (Mount and Louis 2005). Inspired by the work of Wernette et al. (2017), we create a buffer with the radius of the reported positional uncertainty around pairs of shorelines and interpreted the area of intersection between buffers as the joint area of uncertain change for both shorelines. The intersection of the joint area of uncertainty and transition polygons normalized by the size of each transition polygon provides the standard uncertainty ratio in the range of [0,1] associated with each polygon and indicates how much of the observed change can be explained due to the joint uncertainty of shoreline delineations. The ratio indicates how much of the observed change is explained due to the joint uncertainty of shoreline delineations. A ratio of zero indicates that the uncertainty of the pair of shorelines accounts for none of the change. A ratio of one indicates the uncertainty of the pair of shorelines may accounts entirely for the change. To find the area of joint uncertainty (AJU) for more than two shorelines, we first calculate the AJU for each consecutive time interval in the temporal extent, merge them, and find the intersection between merged AJU and transition polygons. This procedure is a filtering technique to exclude transition polygons that have an

associated uncertainty ratio of one or greater than a user-defined threshold. The profession lacks a rule to decide this threshold, which is a topic for future research. The value of the threshold is a trade-off between the number and size of transitional polygons. This becomes important in visualising multi-temporal change analysis where increase in the number of shorelines creates a growing number of smaller transition polygons to capture the variability of change. Showing AJU polygons on the map can help the analyst to understand the spatial distribution of uncertainty.

#### 2.2.2. Transect method

393

394

395

396

397

398

399 400 401

402 403

404

405

406

407

408

409

410

411

412

413

414

415

416

417

418

419

420

421

422

423

424

425

426

427

428

429

430

431

432

433

434

435

436

437

438

439

440

441

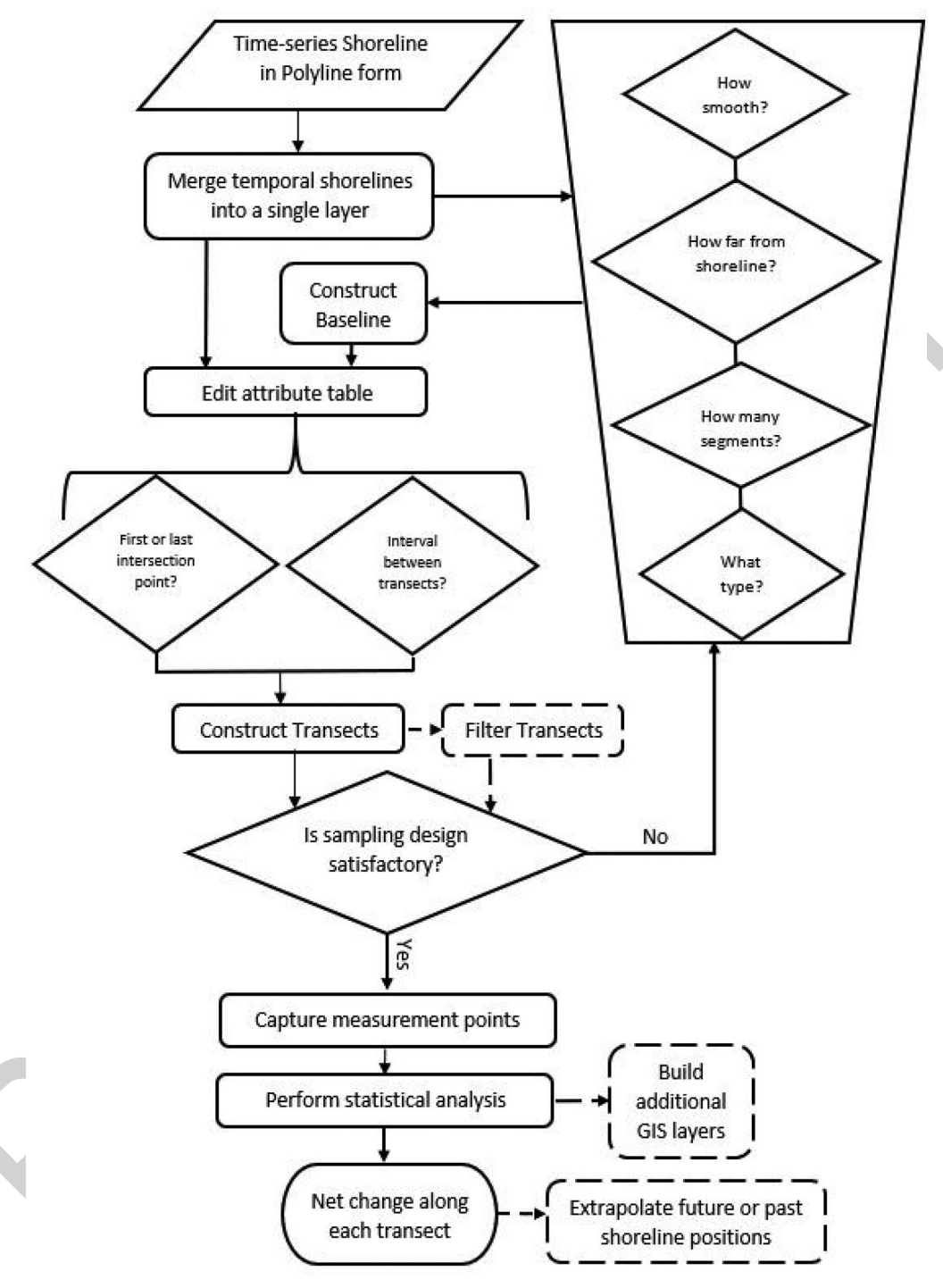
Transect method measures the distance of movement of the polyline boundaries (Jackson et al. 2012). Our literature review showed AMBUR and DSAS are two main freeware packages that implement the Transect method and that researchers use extensively to analyse shoreline change in a vector GIS. The Transect method analyses the movement of edges of a variety of entities such as shorelines, ponds, fires, and ecozones (Jackson et al. 2012). Recently, ESRI added to the ArcGIS Pro sampling toolbox the capability of generating perpendicular transects.

Figure 5 shows the steps to perform the Transect method. This method requires subjective decisions that Table 1 lists and that Figure 5 shows as diamonds. The first step is to construct the baseline layer. The baseline layer is usually created outside the main package with any GIS-capable application and saved as a shapefile or Geodatabase layer. Refer to the AMBUR and DSAS documentation on the official website of these projects for more information on the requirements to make your data analysis-ready.

A baseline is a polyline drawn on either one side or both sides of a time series of shorelines. The baseline should follow the combined orientation of the time series shorelines. Users construct a baseline through either on-screen digitising or automated techniques such as the buffer generation tools in GIS. If the baseline is on land, then the baseline is called onshore, landward or inner. If the baseline is in the water, then the baseline is called offshore, seaward, or outer. The baseline does not necessarily need to be a single polyline and can be defined as a series of polylines that allow the user to choose a particular type of baseline, for example, inner, outer, mid-shore or hybrid for various lengths of the shoreline (Thieler et al. 2009). AMBUR introduced a double baseline, which envelopes the time series of shorelines using both offshore and onshore baselines. Recently DSAS extended the baseline definition by introducing mid-shore baseline, which can be drawn in between shorelines. Both AMBUR and DSAS provide an optional step to smooth the baseline (Jackson et al. 2012; Himmelstoss et al. 2018).

AMBUR uses the baseline and time series of shorelines to construct transects. Transects are straight lines that emanate from the baseline towards the shorelines at userdefined intervals along the baseline. In AMBUR, the user defines the transects' length and casting direction. In the case of a single baseline, transects are cast perpendicular to the tangent of the baseline. Transects are intended to cross all shorelines at the various time points. For double baselines, transects are perpendicular to the offshore baseline and emanate toward the onshore baseline. DSAS v5.0 replaced the idea of fixed length transects with a search radius. Transects are drawn on either side of the baseline and intersect all shorelines within the searching range. This search procedure generates transects that are trimmed to the extent of the shorelines. However, a specific casting direction is still possible for onshore and offshore baselines. The intersection points between transect and shorelines are used to calculate the distance of change along each transect.

The baseline controls each transect's orientation, which influences the coordinates of the intersection points and consequently, affects the distance of temporal change along



**Figure 5.** Flow diagram of the Transect method. Rectangles indicate the required steps. Dashed lines indicate optional steps. Diamonds represent decisions. Trapezoid shows manual operations outside the algorithm.

Table 1. Questions requiring subjective decisions concerning how to draw Baselines and Transects.

501

502

503

504

505

506

507

508

509

510

511

512

513

514

515

516

517

518

519

520

521

522

523

524

525

526 527

528 529

530

531

532

533

534

535

536

537

538

539

Feature	Questions concerning how to draw	
Baseline	What type of baseline should the user choose?	
Baseline	How far from the shorelines should the user draw a baseline?	
Baseline	How smooth should the user draw the baseline?	
Baseline	Should the user choose a single segment or multi-segment baselines?	
Transect	How many transects should the user create?	
Transect	Which intersection point should the user keep when a transect intersects the same shoreline at more than one point?	

each transect. AMBUR and DSAS support perpendicular transects for onshore or offshore baselines. If double baselines are used, then AMBUR supports three additional types of transect casting: trimmed perpendicular, near transect and filtered transect. Trimmed perpendicular transects confine the length of the transect between the onshore and offshore baselines. Near transects are drawn from the offshore baseline to the nearest point on the onshore baseline relaxing the perpendicularity rule. Filtered transects are created using a moving window that averages the azimuth of the casted transects and assigns the averaged value to the middle transect in the window to minimize the gap between transects on the inner baseline in curved shorelines. According to AMBUR developers, these new transect types can mitigate transect overshooting, where a too long fixed-length transect might intersect a shoreline in ferent geographic settings. DSAS achieves the same goal through the search radius. Shoreline sample points are further analysed to estimate the rate of change and to extrapolate the position of a shoreline in the future or past.

AMBUR reports Net Shoreline Movement (NSM) defined as the distance between the transect's intersection points with the shoreline's first and last dates. DSAS reports also the Shoreline Change Envelope (SCE), which is the distance between the most seaward and landward intersection points along each transect. Various techniques exist for computation of the shoreline change rate along each transect. The simplest calculation is the End Point Rate (EPR) where the rate for each transect is the NSM divided by the duration between the dates. This simplicity comes with a price. The EPR model fails to consider the shoreline movement between the first and last dates (Dolan et al. 1991). Compared to other estimators, the EPR becomes more unreliable as the duration between the first and last dates increases. This effect is due mostly to the higher chance of missing cyclic changes. EPR is best suited for calculating the change rate on a short-term basis (Thieler et al. 2009). A Linear Regression Rate (LRR) computes the rate of change along a transect by fitting a least-squares line to describe the distance of shoreline from the baseline as a function of the dates. Each point in the regression derives from the intersection of the transect with the shoreline's time series. The slope of the regression line is the rate of change along each transect accompanied by the standard error of the slope with a confidence interval and R-squared value. The standard error of the estimated position of each shoreline point is also reported (Thieler et al. 2009; Jana 2019). LRR is sensitive to outliers especially when the time-series shoreline is clustered (Dolan et al. 1991). Both AMBUR and DSAS require the users to report the positional uncertainty of each shoreline as part of the attribute table of the time series shoreline dataset. The regression can use weighted linear regression where the weight is a function of each shoreline's uncertainty. The weight for each shoreline is usually the inverse of the squared uncertainty of the shoreline, thus more uncertain shorelines receive smaller weights. AMBUR provides also the least median of squares (LMS) regression in which the median value of the squared residuals determines the regression line. LMS is less sensitive than ordinary least squares regression to outliers. The regression-based techniques and are better than EPR for intermediate or long-term rate of change calculations.

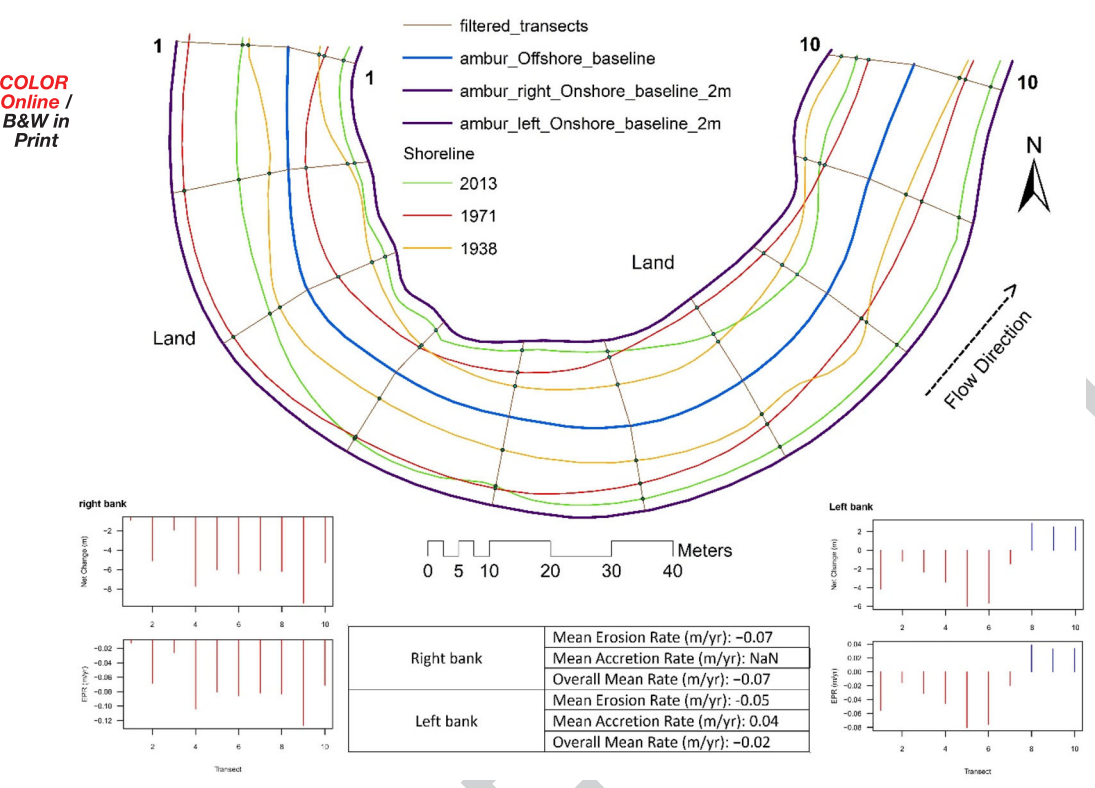


Figure 6. The output from the AMBUR package concerning boundary movement. AMBUR performs the analysis for each riverbank separately using a three-baseline scheme with the offshore baseline common in the analysis of banks. Net change and End Point Rate (EPR) shows erosion for all transects of the right bank. The left bank has seven transects of erosion and three of accretion.

Both packages provide options for shoreline forecasting. DSAS uses a Kalman filter to extrapolate the shoreline position 10 or 20 years into the future accompanied by a polygon layer as an estimation of the positional uncertainty of the extrapolated shoreline and needs at least 4 time points (Himmelstoss et al. 2018; Ciritci and Türk 2020). AMBUR can use EPR, LRR or WLR for the extrapolation.

We used AMBUR to illustrate the Transect method. Figure 6 shows the left riverbank in the north and the right riverbank in the south, where the flow direction determines left and right. We treat each riverbank as its own shoreline. The onshore baseline in the north analyses the northern riverbank. The onshore baseline in the south analyses the southern riverbank. The offshore baseline in the river analyses both riverbanks. AMBUR generates numerous outputs in the form of PDF reports, CSV tables, and shapefiles. Figure 6 summarizes the most informative results. All transects on the right shoreline in the south have loss. For the left shoreline in the north, seven transects have loss and three transects have gain. These results agree with the results of the pairwise overlay of the first and last time points in Figure 7 regarding accretion or erosion on both riverbanks.

#### 3. Results

Table 2 summarizes the characteristics that distinguish between the Area and Transect methods. The Area method measures the area of overlaid polygons. In contrast, the

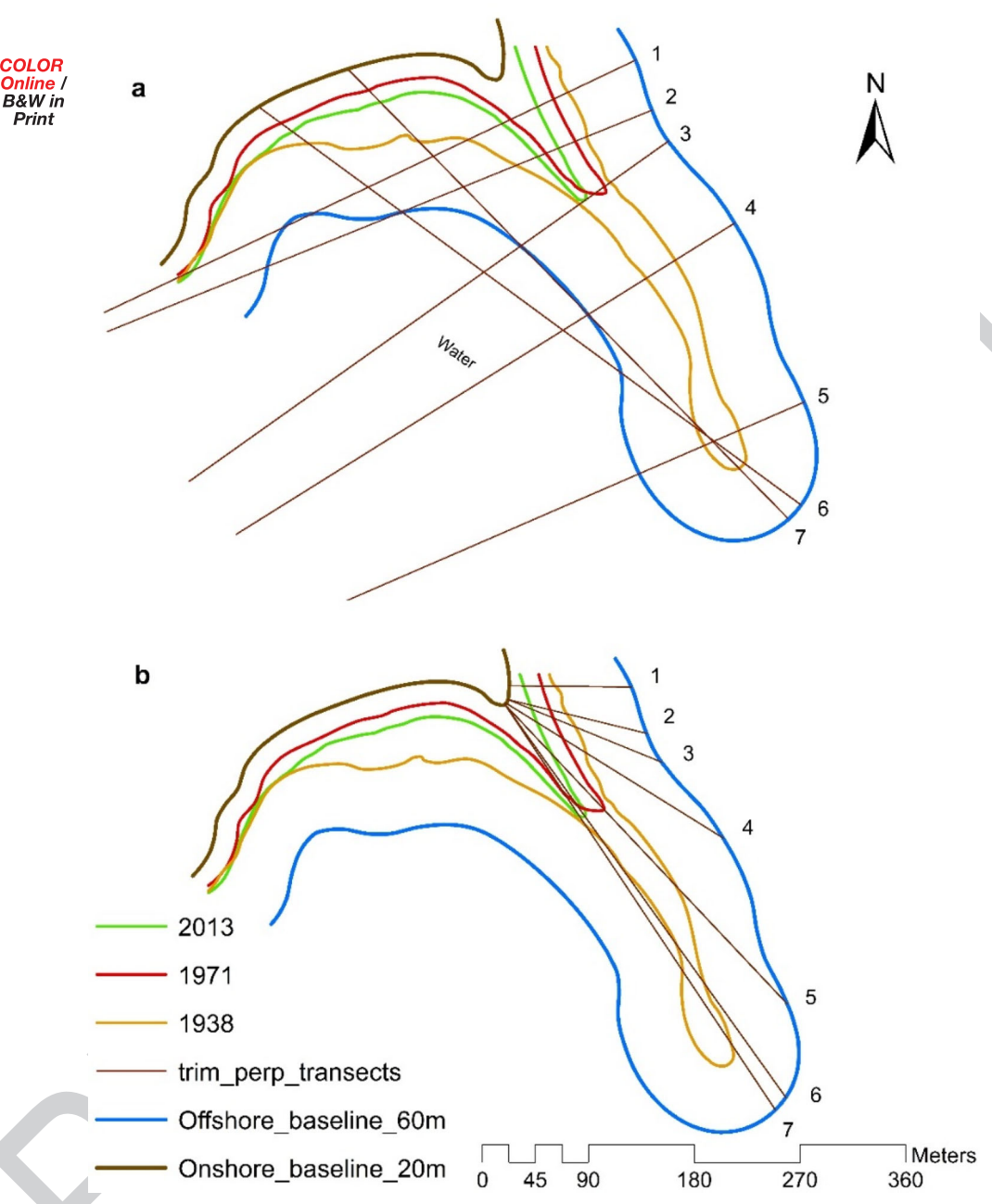


Figure 7. The peninsula's shoreline at 1938 in yellow recedes by 1971 in red, then shifts southeast by 2013 in green. Transects emanate from the offshore baseline towards the onshore baseline. Part a shows trimmed perpendicular transects that either fail to intersect with all the shorelines or have the multiple intersection issue. Part b shows near transects that intersect with all the shorelines but several transects intersect at more than one point on the 1938 shoreline.

Transect method attempts to measure the distance the shoreline has moved through time. The Transect method is a distance sampling strategy that takes samples in equal intervals along emanated transects with the hope that these samples are good representatives to capture the dynamics of the shoreline. modelling the shoreline as a common boundary in

639

642 643 644

645

646 647 648

649 650 651

652 653 654

655 656 657

658 659 660

661 662 663

664 665 666

671 672 673

674 675 676

677 678

679 680 681

682 683 684

685 686

Table 2. Characteristics of the area and the transect methods.

Characteristic	Area Method	Transect Method
Concept to express temporal change	Area	Distance
Data model	Field-based	Object-based
Representation model	Polygon	Polyline
Change type	Gross, Net, Toggle	Net
Works for any curvature of the boundary	Yes	No
Requires parameter tuning	No	Yes
Can predict future boundary	Not automated	Yes
Sensitive to missing data	More	Less
Reports uncertainty	Only visually	Statistical report

Area method uses the whole length of shoreline and doesn't need a sampling strategy hence doesn't require the subjective decisions that influence the Transect method. However, this same advantage becomes problematic in extrapolation of the shoreline future position in as we get a single change rate for the whole length of the spatial extent.

The Area method reports gross loss, gross gain, net and toggle change. The Transect method calculates the net change. For instance, the stacked bar graph in Figure 4 shows 56 m<sup>2</sup>/y of change during the first time interval and 41 m<sup>2</sup>/v of change during the second time interval. Land loss is greater than land gain during both time intervals. Land experiences gross loss of 45 m<sup>2</sup>/year and gross gain of 11 m<sup>2</sup>/year during the first time interval and a gross loss of 32 m<sup>2</sup>/ year and gross gain of 9 m<sup>2</sup>/year during the second time interval. Gross loss is 47 m<sup>2</sup>/year during the temporal extent. Net change is  $-34 \,\mathrm{m}^2/\mathrm{year}$  during the first interval and  $-24 \,\mathrm{m}^2/\mathrm{year}$  during the second interval. Net change is  $-28 \text{ m}^2/\text{vear}$  during the temporal extent.

The curvature of shorelines has no effects on the Area method. However, perpendicular transects can fail to intersect with curved shorelines. Such transects must be discarded or manually edited. Transects 1 to 4 in Figure 7(a) illustrates this problem. Figure 7(b) shows how near transects can overcome this issue by modifying the casting direction but this can give rise to another serious issue of multiple intersection points or result in an arbitrary distance of change along a shoreline.

Each transect must have exactly one intersection point with each shoreline. If a transect intersects a shoreline at more than one point, then the user must decide to use either the most landward or the most seaward intersection point. The decision can influence the rate of change for that transect. Figure 8 illustrates the multiple intersection issue. Transects 1-4 intersect the 1938 shoreline more than once and fail to intersect the shorelines at 1971 and 2013. Transects 5–8 illustrate other forms of the multiple intersection issue.

The constraint of the unique intersection of each transect with a shoreline enforces a separate analysis for each riverbank as shown using a three-baseline design in Section 2.2.2. For the same reason, the Transect method cannot handle temporary islands, which must be removed. Figure 9 shows a situation where an island exists at only 1938. The Area method analyses these situations seamlessly.

Both AMBUR and DSAS provide the associated uncertainty with a confidence interval for the rate of change and the extrapolated position of the shoreline along each transect. We know of no software that automates uncertainty analysis into the Area method. The Area method requires continuous polylines. Any missing part of a shoreline must be filled either manually or through a line-filling algorithm.

#### 4. Discussion

The Transect method requires subject decisions that affect the results. The first decisions concern drawing of the baseline. Baselines should follow the general trend of shorelines,



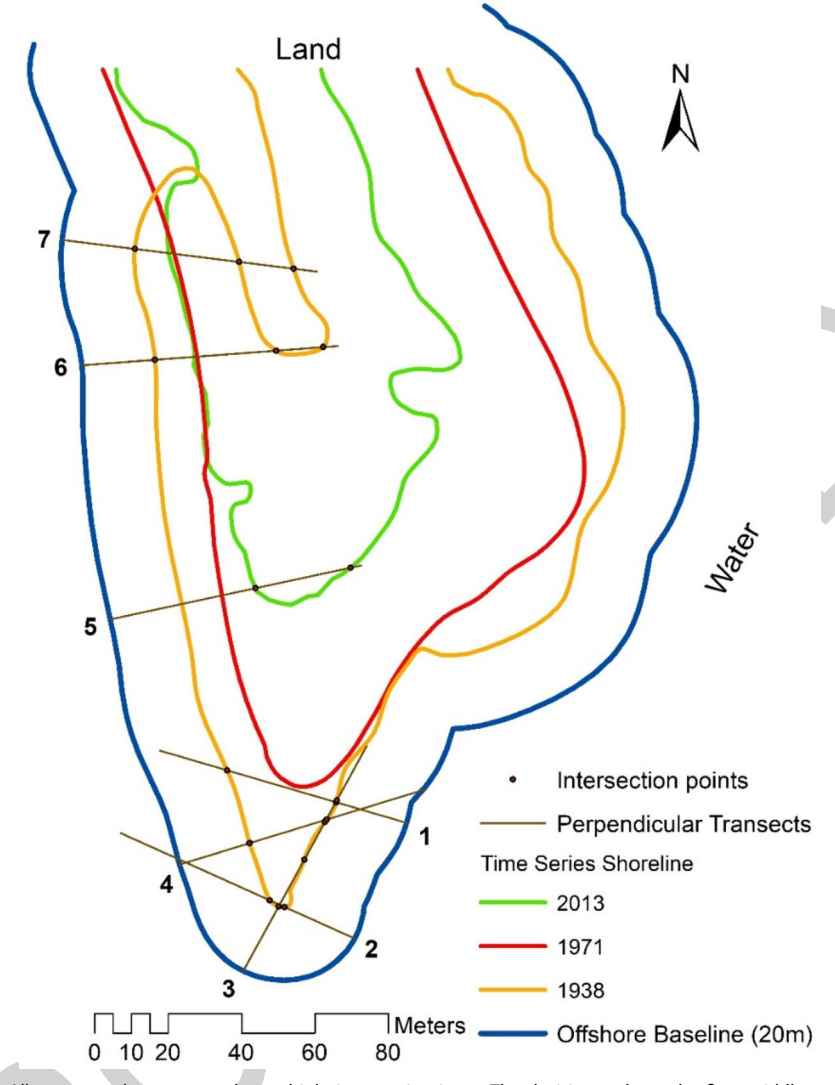


Figure 8. All transects demonstrate the multiple intersection issue. The decision to keep the first, middle, or last intersection point influences the result along these transect. Transects 1-4 are oriented in directions that fail to intersect the shoreline in 1971 and 2013.

meaning the baseline should be approximately parallel to the trend of the shorelines (O'Brien et al. 2014; Himmelstoss et al. 2018). Figures 7 and 8 show how divergence from parallelism between the baseline and shorelines influences the casting direction and the distance between shorelines along transects.

Both AMBUR and DSAS recommend drawing the baseline as close to the shoreline as possible but in the literature we reviewed, this distance is varied between few metres to more than a kilometre. Figures 10 and 11 show how the orientation of each transect varies as a function of the smoothness of the baseline and distance between the baseline and shorelines. Users should avoid smoothing that causes the length of the smoothed baseline to deviate substantially from the original length of the baseline. The combined effect of these arbitrary decisions and the multiple intersection issue can affect the extrapolated position of the shoreline. As a rule of thumb, these subjective decisions can



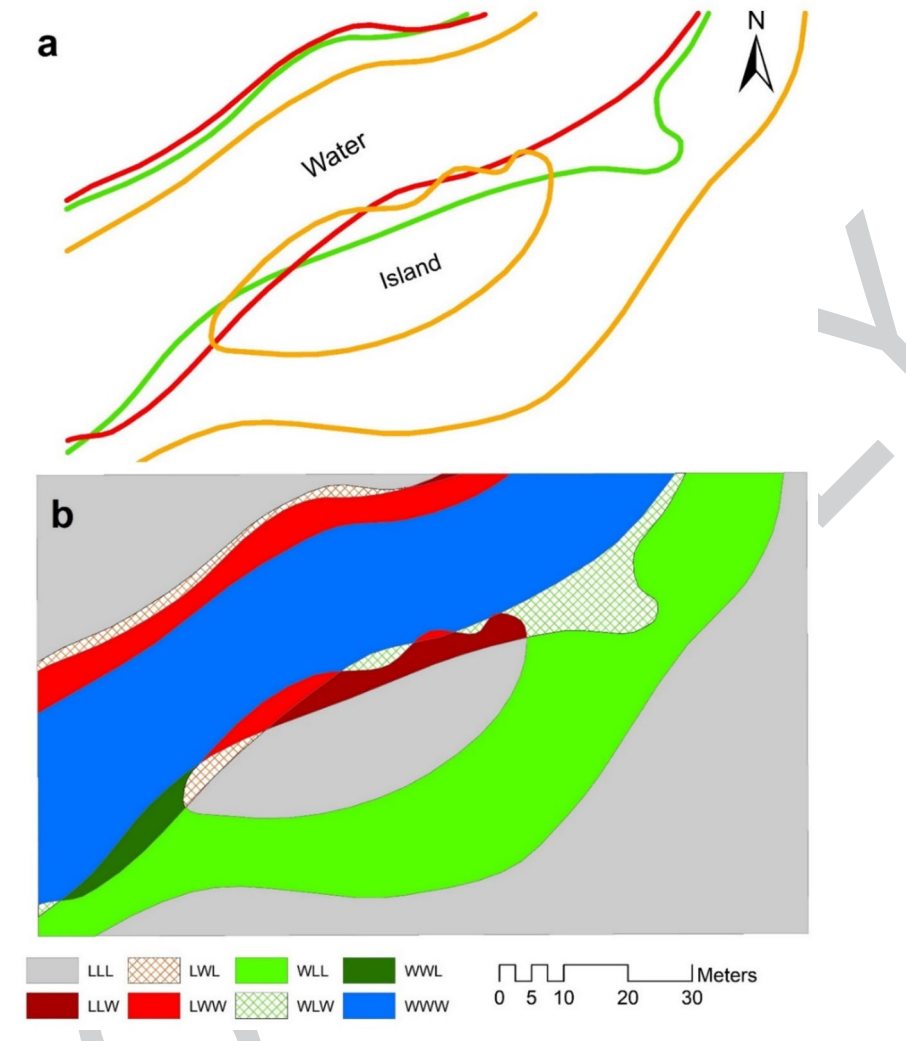


Figure 9. Part a shows a river where an island exists at the year 1938 but at neither 1971 nor 2013. Part b shows the Area method for the same extent.

be safely ignored when the drawn transects meet all the shorelines, transects are approximately perpendicular to the baseline and parallel to each other, and transects are not suffering from the multiple intersection issue. The three-baseline scheme adopted for river networks can mitigate decisions regarding the distance between the baseline and the time series shoreline. Figure 10 shows the difference between near transects cast from the common offshore baseline towards onshore baselines drawn at 2 and 25 metres. Perpendicular transects make the distance decision for onshore baselines irrelevant. However, Figure 12 shows a river segment that has lateral movements that prevent the three-baseline scheme. Figure 12(a) shows a situation where one bank of the river at 1971 intersects the opposite bank at the other time points. Figure 12(b) shows both banks of the river at 1971 moved to one side of the banks at the other time points. AMBUR and DSAS requires the analyst to separate such riverbanks before capturing the intersection points.

Another option is to compute the rate of change based on the movement of the midpoint on a transect between two shorelines. Neither AMBUR nor DSAS compute such

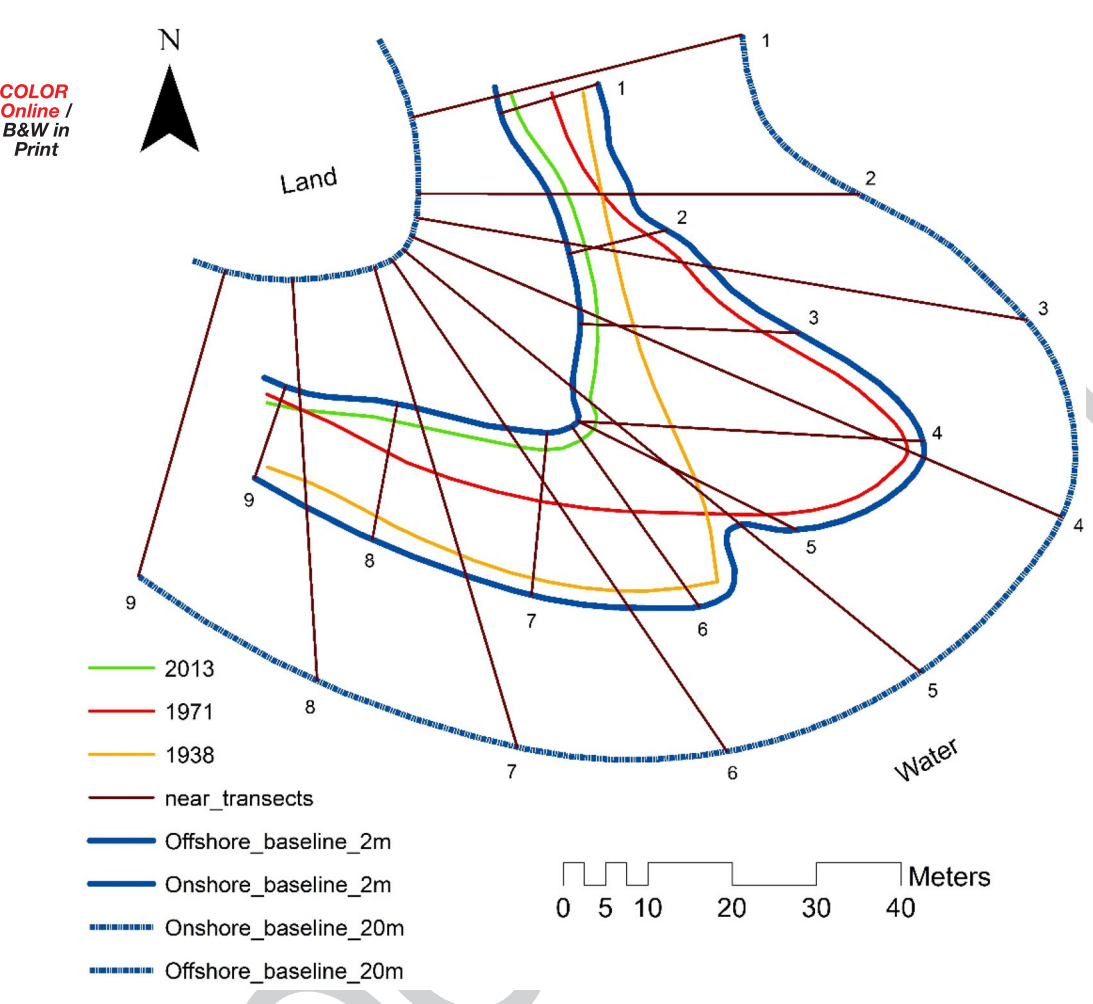
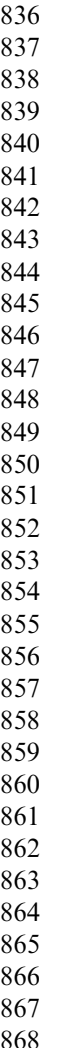
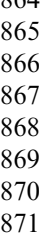


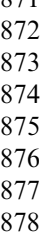
Figure 10. This riverbank segment shows the influence of the distance between shoreline and baselines on the shoreline movement captured by near transects.

mid-points but GIS packages can perform the calculation. Calculating the mid-point for transects affected by multiple intersection issue is tricky and requires manual intervention.

DSAS and AMBUR allow users to organize baseline segments into groups. The number and lengths of baseline segment groups are important decisions. AMBUR and DSAS report statistics for each group of baseline segments. The length of baseline segments together with the transect spacing determines the number of transects from each segment. Users might want to apply a distinct baseline group to each distinct shoreline type, for example, sandy beach, short cliff or manmade structure. A good strategy to design the segments and their grouping is to follow shoreline types or the pattern of land loss and gain via the Area method. Distance between transects should be based on the scale of the shoreline and spatial autocorrelation of change rate between adjacent transects. DSAS version 5.0 uses spatial autocorrelation between transects to adjust the effective sample size in calculating average change rates for each baseline segment group and the entire study region. AMBUR does not provide a mechanism for handling the change rates' spatial autocorrelation between transects.









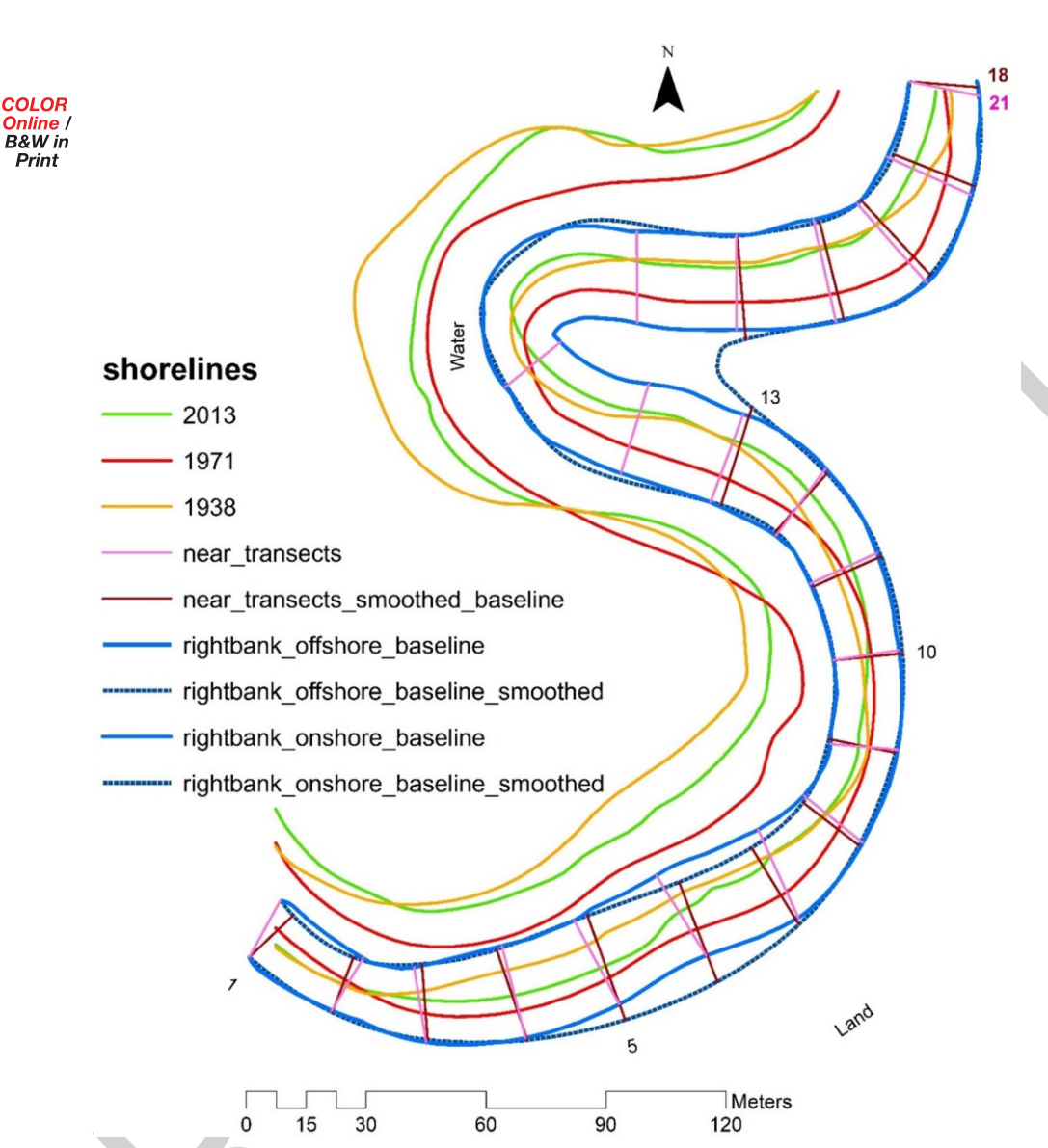


Figure 11. Subjective choices concerning the smoothness of baselines influence the orientation of the transects. Baselines are drawn at 7 metres and near transects are chosen to demonstrate the effect. Simplification of the concave curve after transect 13 eliminates three transects.

DSAS uses perpendicular transects, whereas AMBUR allows perpendicular or non-perpendicular transects. Figure 7(b) shows how each transect's angle from the baseline influences the rate of shoreline movement. Near transects shows promising potential in dealing with curved shorelines. AMBUR uses an optional moving average filter to smooth the deviation from the perpendicular angle for near transects. Users should be aware that the reported distances on the non-perpendicular transect can get two times larger than their perpendicular counterpart when the deviation angle reaches 60 degrees using secant of the deviation angle to convert apparent distance on the inclined transect to its equivalent distance on a perpendicular transect. The definition of distance becomes vaguer as the complexity of the shoreline increases.



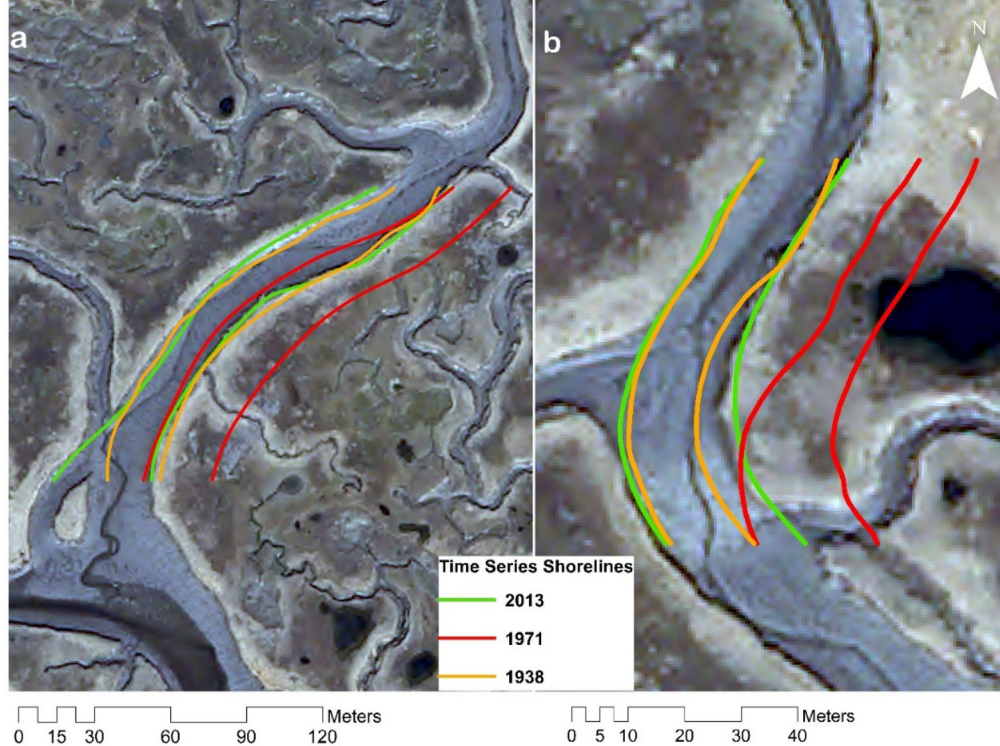
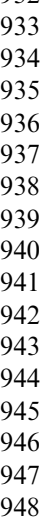


Figure 12. Example of situations where the three-baseline scheme does not work. Part a shows a situation where the west riverbank in 1971 intersects with the east riverbank in 1938 and 2013. Part b shows a situation where both banks in 1971 reside in the east of the banks in 1938 and 2013.

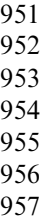
Another important decision is to keep the first or last intersection point for transects that intersect a shoreline more than once. Both packages provide the option to apply a decision for each baseline segment group but not for individual transects from each group. Figure 13 shows how this decision influences movement rates. Figure 13(a) shows that the first point causes most of the analysis envelope to pass over the LWW transition. However, the last intersection point causes most transects to pass through the WLL transition. Exploring how transects pass over transition polygons can raise awareness of the severity of the problem. If the time-series shoreline consists of five or more time points, then users can predict one of the existing shorelines from the rest of the shorelines for the affected transects using either the first or last intersection point then choose the one with the least amount of positional error.

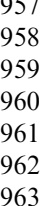
#### 5. Conclusions

The Area method gives results in terms of loss and gain of land area. The concept of land area lost to water and land area gained from water is clear and measurable, therefore, the Area method is straightforward in concept, implementation and interpretation. The Area method reveals the data's patterns, but would require a separate model to extrapolate the shoreline position. The Transect method gives results in terms of net distance of shoreline change and offers a technique for extrapolation. The drawback of the Transect method is its dependence on several subjective decisions concerning how to draw the baseline and transects. Transect method uses subjective decisions to pair a point on an earlier shoreline with a corresponding point on a later shoreline. The concept of distance of shoreline

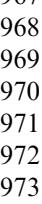
















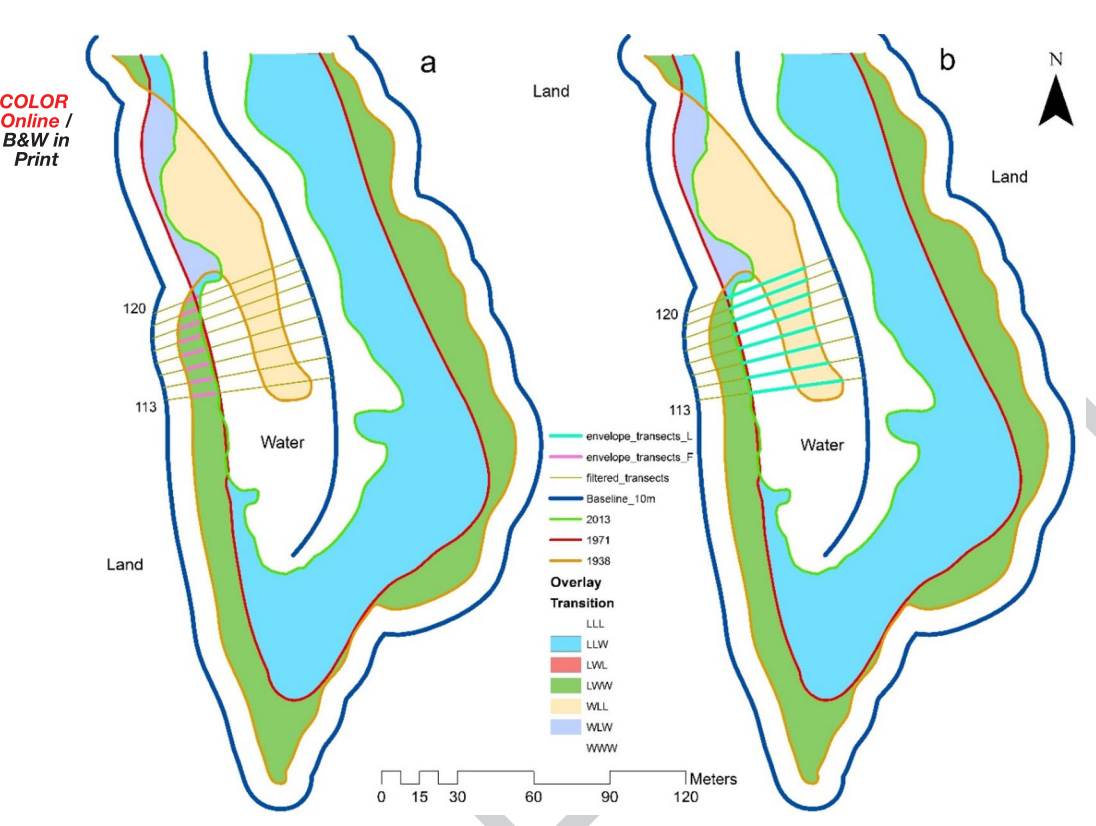


Figure 13. Illustration of the decision concerning whether to keep the nearest or farthest intersection point when transects from the western baseline intersect the 1938 shoreline more than once. Part a shows the length of transects in pink to the nearest intersection point on the 1938 shoreline. Part b shows the length of the transects in cyan to the farthest intersection point.

change becomes especially unclear when the shoreline at one time point is not parallel to the shoreline at another time point, which can occur when peninsulas grow or shrink. The Transect method requires users to make several types of subjective decisions concerning how to draw baselines and transects. Some decisions are more important than other decisions concerning how the decisions influence the results.

Users must align the method with the research question. If the purpose is to examine the loss and gain of land areas, then the Area method offers a straightforward algorithm that many GIS software packages can perform. If the purpose is to measure the net distance that a shoreline moves, then the Transect method is appropriate. This article illustrates boundaries for which the Transect method is difficult or impossible to implement. Therefore, if a user lacks compelling reasons to compute distances, then we recommend the Area method because the concept of area lost and area gained is conceptually clear while the concept of distance of boundary movement is vague.

# **Acknowledgement**

Christine Burns created the data, which the GCE LTER site posted at gce-lter.marsci.uga.edu/data/GIS-GCET-1810.

#### **Authors' contributions**

981 982

983

984

985 986

987 988

989 990 991

992

993 994 995

996

997

998

999

1000

1001

1002

1003 1004 1005

1006

1007

1008

1009

1010

1011

1012

1013

1014

1015

1016

1017

1018

1019

1020

1021

1022

1023

1024

1025

1026

1027

1028

1029

**O**3

Sam Khallaghi conducted the analysis, drafted the article and contributed in conception and interpretation of results. Robert Gilmore Pontius Jr contributed in providing the data, conception and interpretation of results and critically revising the article for important intellectual content.

# Computer code availability

We did not write code for this manuscript.

### **Disclosure statement**

No potential conflict of interest was reported by the author(s).

# Software and data availability

The Applied Coastal Research Laboratory at Georgia Southern University produced a package for the R environment called Analyzing Moving Boundaries Using R (AMBUR) available at http://ambur.r-forge.rproject.org/. Our article uses the open-source AMBUR software to demonstrate the Transect method. The United States Geological Survey produced the Digital Shoreline Analysis System (DSAS), which is freely https://www.usgs.gov/centers/whcmsc/science/digital-shoreline-analysis-system-dsas?qt-science center objects=0#qt-science center objects. DSAS also performs the Transect method. The Area method consists of a few basic steps that various open-source GIS packages can perform. Data are at https://pie-lter.ecosystems.mbl.edu/data.

#### References

O1 Addo KA. 2015. Assessment of the volta delta shoreline change. J Coast Zone Manag. 18. https://doi.org/ 10.4172/2473-3350.1000408. O2

Beetham EP, Kench PS. 2014. Wave energy gradients and shoreline change on Vabbinfaru platform, Maldives. Geomorphology. 209:98-110.

Boak EH, Turner IL. 2005. Shoreline definition and detection: a review. J Coast Res. 214:688-703.

Bracewell J. 2017. Standard operating procedure SHR07: change calculation, data analysis, and reporting Version 1.0 (Standard Operating Procedure). Lafayette, Louisiana: Gulf Coast Network.

Burns CJ, Alber M, Alexander CR. 2020. Historical changes in the vegetated area of salt marshes. Estuaries Coasts.

Calow P, Petts GE, editor. 1992. The rivers handbook: hydrological and ecological principles: in two volumes. Oxford, Boston: Blackwell Scientific Publications.

Ciritci D, Türk T. 2019. Automatic detection of shoreline change by geographical information system (GIS) and remote sensing in the Göksu Delta, Turkey. J Indian Soc Remote Sens. 47(2):233-243.

Ciritci D, Türk T. 2020. Assessment of the Kalman filter-based future shoreline prediction method. Int J Environ Sci Technol. 17(8):3801-3816.

Currin C, Davis J, Baron LC, Malhotra A, Fonseca M. 2015. Shoreline change in the new river estuary, North Carolina: rates and consequences. J Coast Res. 315:1069-1077.

Deabes EAM. 2017. Applying ArcGIS to estimate the rates of shoreline and back-shore area changes along the Nile Delta Coast. IJG. 08(03):332-348.

Dewan A, Corner R, Saleem A, Rahman MM, Haider MR, Rahman MM, Sarker MH. 2017. Assessing channel changes of the Ganges-Padma River system in Bangladesh using Landsat and hydrological data. Geomorphology. 276:257-279.

Dolan R, Fenster MS, Holme SJ. 1991. Temporal analysis of shoreline recession and accretion. J Coast Res. 7:723-744.

Elkafrawy SB, Basheer MA, Mohamed HM, Naguib DM. 2020. Applications of remote sensing and GIS techniques to evaluate the effectiveness of coastal structures along Burullus headland-Eastern Nile Delta, Egypt J Remote Sens Space Sci.

**O**4

- 1030 1031
- 1033 1034
- 1035 1036
- 1037 1038 1039
- 1040 1041
- 1042 1043
- 1044 1045
- 1046 1047
- 1048 1049
- 1050 1051
- 1052 1053 1054
- 1055 1056
- 1057 1058 1059
- 1060 1061
- 1062 1063 1064
- 1065 1066
- 1067 1068 1069
- 1070 1071
- 1072
- 1073 1074 1075
- 1076 1077
- 1078

- balloon-based aerial photography, Albemarle-Pamlico Estuarine System, North Carolina, USA: application of balloon-aerial photography. Limnol Oceanogr Methods. 11(4):151-160. 1032
  - Fearnley SM, Miner MD, Kulp M, Bohling C, Penland S. 2009. Hurricane impact and recovery shoreline change analysis of the Chandeleur Islands, Louisiana, USA: 1855 to 2005. Geo-Mar Lett. 29(6):

Eulie DO, Walsh IP, Corbett DR, 2013, High-resolution analysis of shoreline change and application of

- Florsheim JL, Mount JF, Chin A. 2008. Bank erosion as a desirable attribute of rivers. BioScience. 58(6):
- Himmelstoss EA, Henderson RE, Kratzmann MG, Farris AS. 2018. Digital Shoreline Analysis System (DSAS) version 5.0 user guide: U.S. Geological Survey Open-File Report 2018-1179. (Open-File
- Hopkinson CS, Morris JT, Fagherazzi S, Wollheim WM, Raymond PA. 2018. Lateral marsh edge erosion as a source of sediments for vertical marsh accretion. J Geophys Res Biogeosci. 123(8):2444-2465.
- Jackson CW, Alexander CR, Bush DM, 2012. Application of the AMBUR R package for spatio-temporal analysis of shoreline change: Jekyll Island, Georgia, USA. Comput Geosci. 41:199-207.
- Jana S. 2019. An automated approach in estimation and prediction of riverbank shifting for flood-prone middle-lower course of the Subarnarekha river, India. Int J River Basin Manag. 1-19.
- Jayson-Quashigah P-N, Appeaning Addo K, Amisigo B, Wiafe G. 2019. Assessment of short-term beach sediment change in the Volta Delta coast in Ghana using data from Unmanned Aerial Vehicles (Drone). Ocean Coast Manag. 182:104952.
- Kankara RS, Selvan SC, Rajan B, Arockiaraj S. 2014. An adaptive approach to monitor the Shoreline changes in ICZM framework: a case study of Chennai coast. Indian J Mar Sci. 43:7.
- Kuleli T, Guneroglu A, Karsli F, Dihkan M. 2011. Automatic detection of shoreline change on coastal Ramsar wetlands of Turkey. Ocean Eng. 38(10):1141-1149.
- Kummu M, Lu XX, Rasphone A, Sarkkula J, Koponen J. 2008. Riverbank changes along the Mekong River: remote sensing detection in the Vientiane-Nong Khai area. Quat Int. 186(1):100-112.
- Langat PK, Kumar L, Koech R. 2019. Monitoring river channel dynamics using remote sensing and GIS techniques. Geomorphology. 325:92-102.
- Maiti S, Bhattacharya AK. 2009. Shoreline change analysis and its application to prediction: a remote sensing and statistics based approach. Mar Geol. 257(1-4):11-23.
- Mount N, Louis J. 2005. Estimation and propagation of error in measurements of river channel movement from aerial imagery. Earth Surf Process Landforms. 30(5):635-643.
- Mukhopadhyay A, Mukherjee S, Mukherjee S, Ghosh S, Hazra S, Mitra D. 2012. Automatic shoreline detection and future prediction: a case study on Puri Coast, Bay of Bengal, India. Eur J Remote Sens. 45(1):201-213.
- O'Brien K, Deep C, Stocker J, Clear U, Hyde B, Clear U, Barrett J, Grant CS. 2014. Analysis of shoreline change in Connecticut 51.
- Pollard JA, Brooks SM, Spencer T. 2019. Harmonising topographic & remotely sensed datasets, a reference dataset for shoreline and beach change analysis. Sci Data. 6(1):42. https://doi.org/10.1038/s41597-019-0044-3.
- Pontius RG, Krithivasan R, Sauls L, Yan Y, Zhang Y. 2017. Methods to summarize change among land categories across time intervals. J Land Use Sci. 12(4):218-230.
- Rooney J, Fletcher C, Barbee M, Eversole D, Lim S-C, Richmond B, Gibbs A. 2009. Dynamics of sandy shorelines in Maui, Hawaii: consequences and causes.
- Roy S, Mahapatra M, Chakraborty A. 2018. Shoreline change detection along the coast of Odisha, India using digital shoreline analysis system. Spat Inf Res. 26(5):563-571.
- Sarwar MGM, Woodroffe CD. 2013. Rates of shoreline change along the coast of Bangladesh. J Coast Conserv. 17(3):515-526.
- To DV, Thao TP. 2008. A shoreline analysis using DSAS in Nam Dinh coastal area. Int J Geoinformatics.
- Vos K, Splinter KD, Harley MD, Simmons JA, Turner IL. 2019. CoastSat: a google earth engine-enabled python toolkit to extract shorelines from publicly available satellite imagery. Environ Model Softw. 122:
- Wernette P, Shortridge A, Lusch DP, Arbogast AF. 2017. Accounting for positional uncertainty in historical shoreline change analysis without ground reference information. Int J Remote Sens. 38(13): 3906-3922.
- Wiberg PL, Taube SR, Ferguson AE, Kremer MR, Reidenbach MA. 2019. Wave attenuation by oyster reefs in shallow coastal bays. Estuaries Coasts. 42(2):331-347.

Yao Z, Ta W, Jia X, Xiao J. 2011. Bank erosion and accretion along the Ningxia-Inner Mongolia reaches of the Yellow River from 1958 to 2008. Geomorphology. 127(1-2):99-106.

- Zagórski P, Jarosz K, Superson J. 2020. Integrated assessment of shoreline change along the Calypsostranda (Svalbard) from remote sensing, field survey and GIS. Mar Geod. 43(5):433-471.
- Zeinali S, Talebbeydokhti N, Dehghani M. 2020. Spatiotemporal shoreline change in Boushehr Province coasts. J Ocean Limnol. 38(3):707-721.
- Zhu L, Wu J, Xu Z, Xu Y, Lin J, Hu R. 2014. Coastline movement and change along the Bohai Sea from 1987 to 2012. J Appl Remote Sens. 8(1):083585. .